15th International Symposium on Computer Methods in Biomechanics and Biomedical Engineering
and
3rd Conference on Imaging and Visualization
CMBBE 2018
P. R. Fernandes and J. M. Tavares (Editors)

PECTOPEXY TO REPAIR VAGINAL VAULT PROLAPSE: A FINITE ELEMENT APPROACH

Aroj Bhattarai* **and Manfred Staat†**

Biomechanics Laboratory, Institute of Bioengineering, FH Aachen University of Applied Sciences
Heinrich-Mußmann-Str.1, 52428, Jülich, Germany
bhattarai@fh-aachen.de, staat@fh-aachen.de

Keywords: Prolapse, pectopexy, mesh implant, biomechanical modeling.

Abstract: *The vaginal prolapse after hysterectomy (removal of the uterus) is often associated with the prolapse of the vaginal vault, rectum, bladder, urethra or small bowel. Minimally invasive surgery such as laparoscopic sacrocolpopexy and pectopexy are widely performed for the treatment of the vaginal prolapse with weakly supported vaginal vault after hysterectomy using prosthetic mesh implants to support (or strengthen) lax apical ligaments. Implants of different shape, size and polymers are selected depending on the patient's anatomy and the surgeon's preference. In this computational study on pectopexy, DynaMesh®-PRP soft, GYNECARE GYNEMESH® PS Nonabsorbable PROLENE® soft and Ultrapro® are tested in a 3D finite element model of the female pelvic floor. The mesh model is implanted into the extraperitoneal space and sutured to the vaginal stump with a bilateral fixation to the iliopectineal ligament at both sides. Numerical simulations are conducted at rest, after surgery and during Valsalva maneuver with weakened tissues modeled by reduced tissue stiffness. Tissues and prosthetic meshes are modeled as incompressible, isotropic hyperelastic materials. The positions of the organs are calculated with respect to the pubococcygeal line (PCL) for female pelvic floor at rest, after repair and during Valsalva maneuver using the three meshes.*

1. INTRODUCTION

Obesity is associated with an increased risk for genital prolapse [1], the sigmoid colon enlarged by fatty tissue provides less space for sacrocolpopexy. In obese patients, the mesh implanted between the sacrum and the vagina/cervical stump narrows the pelvis, which might result in defecation disorders, adhesions, or trauma of the hypogastric nerves [2]. Introduced for the first time in 2007 [3], laparascopic pectopexy minimizes such risks and has rapidly emerged as a promising technique for the prolapse repair in obese patients with good postoperative outcomes. This method uses the lateral parts of the iliopectineal ligament (Cooper ligament) for a bilateral mesh fixation [4]. The mesh implant carefully follows the direction of the round and broad ligaments without crossing or interfering sensitive areas such as the ureter, bowel or hypogastric trunk which offers zero restriction to the organ function by the implant. In this way, fixation at the stable and significantly stronger iliopectineal ligament than the sacrospinous ligament and arcus tendinous fasciae pelvis ensures a more physiological axis of the vagina [4], [5].

In this study, we intended to investigate the biomechanical performance of the pectopexy after hysterectomy to correct an apical prolapse using a 3D finite element model of the female pelvic floor. Implant models are included in the pelvic floor model to examine the effectiveness of DynaMesh®-PRP soft (FEG Textiltechnik mbH, Aachen, Germany), GYNECARE GYNEMESH® PS Nonabsorbable PROLENE soft® (Ethicon, USA)[1] and Ultrapro® (Ethicon, USA) mesh implants to correct apical prolapse by lifting the vaginal cuff. Simulations are conducted with lax tissues modeled by reducing their stiffness to simulate the weakened pelvic floor during prolapse. The positions of the organs and the vaginal axis are calculated at rest, after surgery and during Valsalva maneuver. The results of the finite element analyses presented in this study serve to compare different prosthetic devices used for pectopexy. The results obtained are later compared with our other findings for sacrolpopexy repair [6].

2. Materials and methods

2.1 Pectopexy mesh implant

The computational model of the pectopexy mesh implant is based on the specifications of the DynaMesh®-PRP soft mesh implant of FEG Textiltechnik mbH, Aachen, Germany (Figure 1). The PVDF fiber diameter ($\phi_{\text{fiber}} = 103.8\mu\text{m}$) and the mesh thickness ($\phi_{\text{longitudinal}} = (333.6 \pm 36.2)\mu\text{m}$ and $\phi_{\text{transversal}} = (174.2 \pm 21.7)\mu\text{m}$) as shown in the right red panel in Figure 1 are measured using the digital VHX-600 microscope (Keyence, Japan) [7]. The implant is modeled as a rectangular strip which is broader in the center and at its sides. The broader parts are used to fix the implant to the vaginal stump as well as the left and right iliopectineal ligament with sutures (Figure 1).

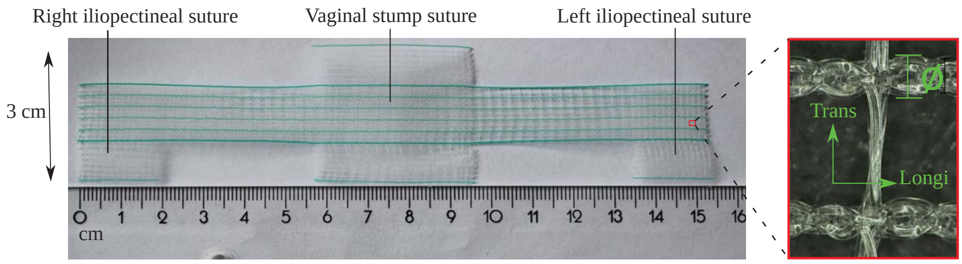

Figure 1: Dimensions of a standard DynaMesh®-PRP soft mesh implant where the right red panel represents a higher magnification view of the red square on the left panel showing PVDF polymer fibers using a digital microscope VHX-600 (Keyence, Japan).

2.2 Female pelvic floor model from plastination technique

A three dimensional biomechanical model of the female pelvic floor was constructed from a pelvis of a 70-year old cadaver based on the standard ultra-thin slice plastination technique [8], [9]. Slices of 1.5 mm thickness cut from the frozen block of the pelvis were dehydrated, fat freed and hardened to construct high quality and perfectly transparent epoxy (E12) slices (Figure 2a).

[1] Subsequently GYNECARE GYNEMESH® PS Nonabsorbable PROLENE soft® is also abbreviated as Gynemesh®.

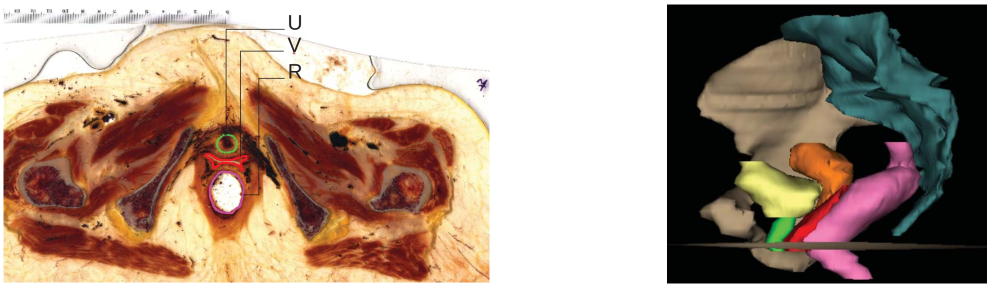

(a) (b)

Figure 2: a) Epoxy (E12) slice number 7 of the female pelvis in WinSURF software (2D tool) [8], b) 3D computer model constructed using WinSURF software (3D tool) with a gray horizontal plane at the level of the 2D slice number 7 on the left. U = Urethra (green); V = Vagina (red); R = Rectum (pink).

2.3 Volume rendered model from E12 slices

The finished E12 slices were scanned from both sides using an EPSON GT-10000+ Color Image Scanner with 600 dpi. Scanned images of the plastinated tissue slices were imported as BMP files and were loaded into the WinSURF[2] software for reconstruction. Each structure which need to be reconstructed was manually traced on every slice with a graphic table (Wacom Cintiq 24HD). For example, in Figure 2a the manually drawn green, red and pink curves outline the urethra, vagina and rectum, respectively. The reconstruction was rendered and visualized as a 3D model (Figure 2b) and subsequently transformed into the .OBJ format. The UTHSCSA (University of Texas Health Science Center in San Antonio) IMAGE TOOL v.2.0[3] was used to morphological measure the pelvic structures and distance between them [8].

Pre-smoothing and repairing of holes in the visualized model (Figure 2b) after 3D reconstruction is done by using the 3D mesh processing software MeshLab[4]. Other artefacts such as distorted elements (aspect ratio, angular and volumetric) are hard to map onto physical coordinates. Also, finite element (FE) simulations with a lot of distorted elements and/or extreme deformations may have problems to converge [10]. Therefore, the Rhino software[5] is used to repair and transform the irregular surfaces into smooth free-form surfaces based on non-uniform rational B-splines (NURBS) as shown in Figure 3. NURBS are easier to handle, robust in defining physical coordinates of irregular morphology and produce smooth surfaces for FE mesh generation. The detailed methodology of creating a 3D model from plastinated slices has been described in [6], [9].

2.3.1 Three dimensional FE mesh

The smoothed geometries are then imported into the open source pre- and post-processing software Salome[6]. The pre-processing is done with the GEOM (geometry) module of Salome and is used to exchange data between CAD and FEM software (Figure 3). It can also be used to create geometries of an arbitrary shape. Considering the thickness of pelvic organs, ligaments,

[2] `www.surfdriver.com` [3] `compdent.uthscsa.edu/dig/itdesc.html` [4] `www.meshlab.net`
[5] `www.rhino3d.com` [6] `www.salome-platform.org`

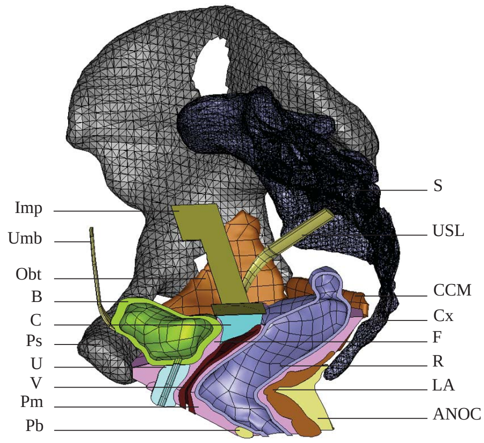

Figure 3: Sagittal section of the female pelvic floor showing the smoothed NURBS-based geometry. The mesh implant suspends the cervical stump after hysterectomy from the iliopectineal ligament. The rigid pelvic bone is included to show the attachment of the pelvic muscles, fasciae and ligaments for organs. ANOC = Anococcygeal raphe; USL = Uterosacral ligament; Umb = Umbilical ligament; Pm = Perineal membrane; Pb = Perineal body; F = Endopelvic fascia; CCM = Coccygeus muscle; LA = Levator ani muscle; Obt = Obturator internus muscle; B = Bladder; V = Vagina; U = Urethra; R = Rectum; C = Cervical stump; Imp = PRP-soft implant; PS = Pubic symphysis; Cx = Coccyx; S = Sacrum.

muscles, fasciae and mesh implant, we adopt a volume discretization to generate 3D meshes. Finally, a smooth compound FE mesh of the female pelvic floor is generated which consists of 611,798 linear tetrahedrons (4 node elements). In addition, the vaginal body was modeled using 28,833 quadratic tetrahedrons with 6 additional nodes, one at the middle of each edge for higher precision of contact simulations.

2.4 Mechanical modeling of pelvic structures and mesh implant

2.4.1 Pelvic tissues

An appropriate modeling of the soft tissue mechanical response is of critical importance. For such materials, neither the force-elongation nor the stress-strain/stretch relation agrees with the linearly elastic Hooke's law. Macroscopically, for such materials, the highly non-linear, incompressible and elastic stress-strain/stretch relation can be derived using the *Helmholtz free-energy function* (W) per unit reference volume, which is referred as the isotropic strain energy function (SEF) [11]. In uniaxial tension a three parameter Mooney Rivlin model is

$$W = C_{10}\Big(\lambda^2 + \frac{2}{\lambda} - 3\Big) + C_{01}\Big(2\lambda + \frac{1}{\lambda^2} - 3\Big) + C_{20}\Big(\lambda^2 + \frac{2}{\lambda} - 3\Big)^2 - p\Big(J - 1\Big), \quad (1)$$

where C_{10}, C_{01} and C_{20} are the material parameters with dimensions of stress (MPa), p is an indeterminate *Lagrange multiplier* identified as a hydrostatic pressure which can be determined from the equilibrium equations, λ is the stretch in uniaxial tension for an incompressible material and the Jacobian $J := \det[\mathbf{F}]$ is the determinant of the deformation gradient tensor $\mathbf{F}$.

2.4.2 Mesh implants

The industrial project partner FEG Textiltechnik mbH provided force-elongation data for three well-known meshes (DynaMesh®-PRP soft, Gynemesh® and Ultrapro®) which have been tested on an uniaxial tensile machine and are used in this FE model for prolapse repair. The stress-stretch curves have been derived from the force-elongation curves of the mesh implants [6] which show either nearly linear or non-linear orthotropy depending on the mesh structure and its pore deformation. For DynaMesh®-PRP soft with regular rectangular pores (Figure 1), nearly linear elastic orthotropy is observed. Therefore, the Young's modulus is computed for each mesh in longitudinal (E_L) and transversal (E_T) direction (Table. 1). The Poisson's ratio (ν_{LT}) and shear modulus (G_{LT}) for the DynaMesh®-PRP soft implant have been adopted from the structurally similar Parietex mesh which have been determined by Staat et al. [12]. On the other hand, the Gynemesh® and Ultrapro® with its large pore deformation along the loaded direction

Structure	C_{10} (MPa)	C_{01} (MPa)	C_{20} (MPa)	References
Pelvic tissues				
Uterosacral	1.6	-	8.0	[13]
Cardinal, Perineal body	0.2288	-	1.144	[14]
Pubourethral	0.68	-	5.0	[13]
Uterus, Vagina	0.4	-	3.2	[15]
Rectum	0.73	-	1.4	[15]
Vesica, Urethra	0.0835	-	0.092	[16]
Fascia, Perineal membrane	0.00079515	0.000486388	0.01216	[17], [18]
Pelvic muscle	0.0625	-	-	[19]
Mesh implants				
Gynemesh®	0.9	0.25	1.75	
Ultrapro®	0.1	-	5.85	
	E_L(MPa)	E_T(MPa)	ν_{LT}	G_{LT} (MPa)
DynaMesh®-PRP soft	46.859	3.573	0.07	4.37

Table 1: Biomechanical properties of female pelvic structures fitted with three term polynomial function on stress-strain curves from listed literature. Implants are parameterized using equation (1). For further detail, the reader may refer to [6].

show significantly non-linear mechanical behavior. The stress-stretch curves for Gynemesh® along the longitudinal and transversal load directions are quite similar. The Ultrapro® showed distinct non-linear orthotropy with higher stiffness along the longitudinal direction. The isotropic hyperelastic Mooney Rivlin model (Equation 1) is used to model the mechanical behavior of the implants. The material parameters are listed in Table 1.

2.4.3 Parameter identification

The stress-strain curves of the pelvic structures are adopted from different experiments published in the literature. They are fitted with the Mooney Rivlin type model (Equation 1) to obtain isotropic hyperelastic parameters (Table 1) which have been used in different numerical studies [6], [18]. The stress-strain response of the mesh implants vary from nearly linear

(DynaMesh®-PRP soft) to nonlinear (Gynemesh® Prolene soft and Ultrapro®). The *linearly elastic orthotropic* and *isotropic hyperelastic material models* are used to characterize the mechanical behavior.

2.5 Boundary conditions

The surfaces of the pelvic muscles, the ligaments and the endopelvic fascia attached to the pelvic bone are fixed. Bones shown in Figure 2 are rigid structures and are not included in the simulation. An intra-adbominal pressure (IAP) of 4 kPa during supine Valsalva maneuver[7] is applied on the upper surface of the organs [20]. The inner surface of the bladder is subjected to a fluid pressure of 600 mm H_2O = 5.8 kPa. Based on the *Integral Theory*, the lateral vaginal wall transmits muscle contractions against suspensory ligaments; the levator ani muscle pulls the vagina posteriorly and inferiorly against the apical ligaments [21].

Weakened tissues fail to maintain the normal position of the organs [6], [19], [18] which can be well stabilized by using mesh implants fixed to the iliopectineal ligaments on each sides (Figure 2). The proximal ends of the pectopexy implant model follows the continuity of the round and the broad ligament of the uterus. The implant is fixed to a segment of the iliopectineal ligament in between the insertion of the iliopsoas muscle and the obturator canal [4]. The distal end of the pectopexy implant is attached to the cervical stump in a tension-free manner. This situation of the pelvic floor is considered the resting state in the numerical study. Later, pelvic organ movement is simulated under increased IAP during Valsalva maneuver. A mesh implant with good mechanical behavior holds the organs in their desired position.

3. Biomechanical simulation of pectopexy

The FE simulation of the deformation and the pectopexy treatment using prosthetic mesh implants are performed with the open source software, *Code_Aster*[8]. Using parallel solver technology on a Linux-based multi-core processor, each simulation took about 5 hours and 30 minutes with two Intel Xeon processors (8 core, 3.10GHz Turbo, 20MB, 8.0 GT/s).

The biomechanical simulation results of the symptomatic pelvic floor after pectopexy surgery at rest and during Valsalva maneuver are shown in Figure 4. After the surgical intervention with the use of pectopexy mesh implants suspended bilaterally to the iliopectineal ligament, the stability of the organ positions is expected to be similar to other prolapse repair techniques, for example sacrocolpopexy. Bhattarai et al. [6] simulated the pathophysiological phenomena of the vaginal cuff prolapse and sacrocolpopexy repair after hysterectomy using a Y-shaped DynaMesh®-PRS soft implant model. The results of the prolapse and the sacrocolpopexy repair (Figure 5) have been validated with respect to the organ positions measured from the pubococcygeal line (PCL) drawn in the MRI scans of a female patient with prolapse after hysterectomy (Table 2). Most researchers in radiography adapt the PCL line between the inferior symphysis pubis and the last visible coccygeal joint for the quantification of the prolapse.

In this study, anatomical symptom of the vaginal cuff prolapse is significantly stabilized with pectopexy as well. Using the mesh type DynaMesh®-PRP soft, the bladder base (13.12 mm) and

[7] It is characterized by a forced exhalation against a closed glottis which suddenly increases the intra-abdominal and intrathoracic pressures due to the contractions of the abdominal and respiratory muscles.
[8] `http://www.code-aster.org`

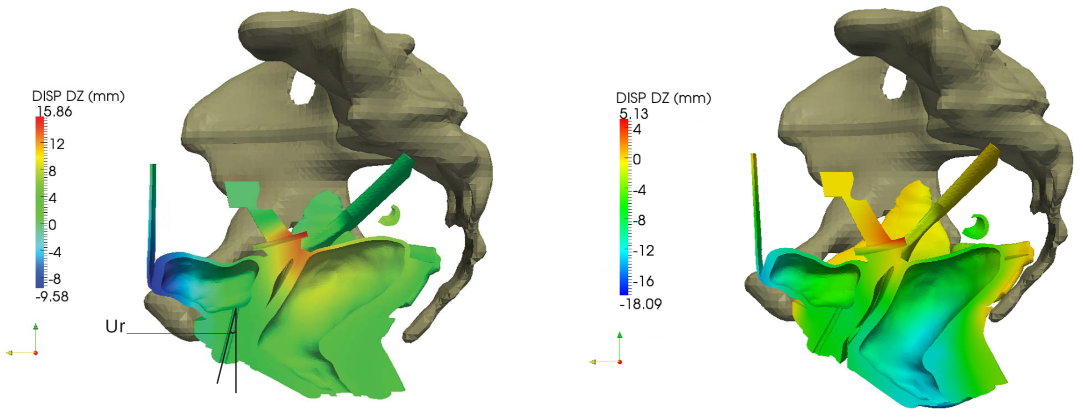

(a) (b)

Figure 4: Finite element simulation of the pectopexy surgery showing the organ positions after hysterectomy a) at rest, after surgery to suspend cervical cuff at iliopectineal ligament using DynaMesh®-PRP soft implant and b) during Valsalva maneuver. Positions of the cervical cuff, bladder and urethral axis are compared. The change of the urethral axis is measured by angle Ur (°) with vertical line.

the vaginal cuff (36.45 mm) post-pectopexy at rest are repositioned well above the PCL line (Figure 4a). The two other meshes: Gynemesh® and Ultrapro® are also tested. For both these meshes, the lifting of the bladder base shown by # in Figure 5 is just above the PCL line due to their mechanical behavior. The vaginal cuff (*) is lifted high above the PCL line and is directed towards S4 sacrum bone. Comparing the three meshes, DynaMesh®-PRP soft is found to be functionally stable since the new orientation of the vaginal axis is along the anatomical direction of the uterosacral ligament (or S2 bone) which normally occurs in the healthy pelvic floor.

The correction of the dislocated pelvic organs during Valsalva maneuver is important because the critical dislocation may affect their function. The overall success of the pectopexy surgery allows the significant organ movement under increased intra-abdominal pressure that is governed by mesh elasticity. The displaced position of the organs after pectopexy with the

	Sacrocolpopexy [6]			Pectopexy		
	P_{Bb} (mm)	P_{VC} (mm)	Ur (°)	P_{Bb} (mm)	P_{VC} (mm)	Ur (°)
Prolapse	-9.19	-10.03	36.74°	-	-	-
DynaMesh®-PRS soft	9.23	37.24	8.17°	-	-	-
DynaMesh®-PRP soft	-	-	-	-4.37	15.31	28.5°
Gynemesh®	2.3	27.12	26.28°	-8.75	5.10	33°
Ultrapro®	1.25	25.72	27.43°	-10.21	4.37	34°

Table 2: Measurement of the bladder base, vaginal cuff and urethral axis during Valsalva maneuver for sacrocolpopexy [6] and pectopexy repair simulations using the mesh types DynaMesh®-PRS soft and DynaMesh®-PRP soft, respectively. Positive values represent the distance measured above the PCL line and negative values represent the distance measured below the PCL line.

use of DynaMesh®-PRP soft mesh during Valsalva maneuver is shown in Figure 4b and Figure 5. Compared to the prolapse movement simulated in Bhattarai et al. [6], anatomical symptom of vaginal vault prolapse is significantly modified. In contrast, the pectopexy results are moderate compared to the sacrocolpopexy technique (Table 2). Nevertheless, the lifted position of the vaginal cuff (DynaMesh®-PRP soft: 15.31 mm, Gynemesh®: 5.10 mm and Ultrapro®: 4.37 mm above PCL) post-pectopexy demonstrates the success of all meshes. However, the bladder base and the urethro-vesical junction is not well supported above the PCL line under Valsalva maneuver. The distance of the bladder base above the PCL is measured to be -4.37 mm for the DynaMesh®-PRP soft and -8.75 mm and -10.21 mm for the Gynemesh® and the Ultrapro® meshes, respectively.

In addition, the DynaMesh®-PRP soft is also found to stabilize the urethral axis, Ur (28.5°) better than the Gynemesh® and the Ultrapro® (≈ 34°). Bladder hypermobility and an urethral axis, Ur > 30° are considered to be symptomatic for stress urinary incontinence [18], for example 36.74° in prolapse situation [6].

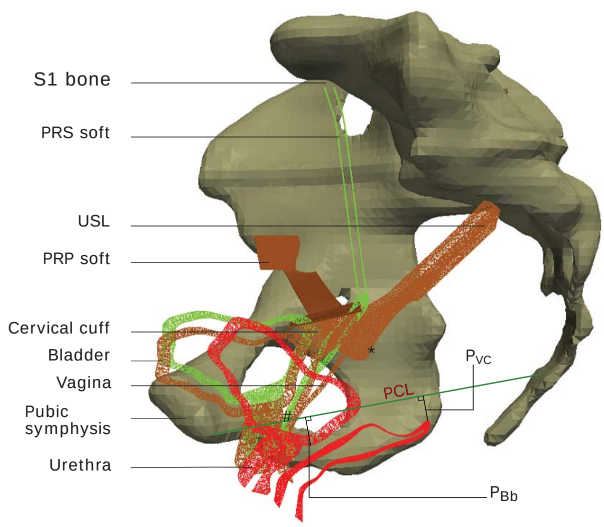

Figure 5: Sagittal slices measuring the bladder base (P_{Bb}) and the vaginal cuff (P_{VC}) from the PCL (green) line. Red structures show the simulated vaginal vault prolapse. Green and brown structures show sacrocolpopexy (using DynaMesh®-PRS soft implant) and pectopexy (using DynaMesh®-PRP soft implant) simulations, respectively at rest.* and # show the positions of the vaginal cuff and bladder base for pectopexy using Ethicon meshes.

4. Discussions and Conclusions

Pelvic organ prolapse is a common complication in multiparous elderly women caused by a weakening, laxity or reduced stiffness of the supporting network of pelvic muscles, ligaments and connective tissues which hold the pelvic organ after menopause [16], [22], [23], [24]. Vaginal vault prolapse is the descent of the vaginal apex or cuff scar which can occur either in combination with uterine prolapse or post-hysterectomy (up to 40%), after surgical removal of the uterus, and can coexist with the prolapse of the bladder (cystocele), urethra (urethrocele), rectum (rectocele) or small bowel (enterocele) [25]. Various operative approaches such as sacrocolpopexy, sacrospinous/iliococcygeus fixation and pectopexy for the repair of a genital prolapse have been reported [3], [26], [27], [28] [29], [30]. The choice of operation depends on the patient's age, severity of the prolapse, postoperative mesh related complications, co-morbidity, previous surgery, the level of physical and sexual activity and the experience of the surgeon [31].

Laparoscopic sacrocolpexy is considered to be the gold standard to correct the apical prolapse and to obtain a reconstitution of the physiological vaginal axis [6], [27]. However, it is highly posed to intraoperative presacral hemmorrhage [32] and reduced pelvic space [2].

Complications are chronic pain, defecation disorders, stress urinary incontinence and adhesion or injury of hypogastric nerves specially in obese populations [2], [33]. Similarly, for sacrospinous/iliococcygeus fixation, complications associated are hemorrhage, cystocele (20-30%), perforation of bladder, rectum or small bowel, buttock pain, voiding dysfunction and ischiorectal abscess, perineal hernia and necrotizing infection [28] [29], [30], [34].

As obesity is associated with an elevated risk for genital prolapse [1], the sigmoid colon enlarged by fatty tissue provides less space for sacrocolpopexy. Thus, laparascopic pectopexy is a good alternative for the treatment of vaginal vault prolapse in obese patients. It adapts the benefits of laparoscopy on obese patients with a difficult surgical pelvis [3] who are thought to be at higher risk of defecation disorders and lateral cystocele with conventional techniques of prolapse repair (sacrocolpopexy and sacrospinous/iliococcygeus fixation) [4]. Performed with the minimally invasive technique this method allows the lateral parts of the statistically stronger iliopectineal ligament for a bilateral fixation of the vaginal cuff after hysterectomy [5]. The medial parts of this ligament have been used successfully for Burch colposuspension and lateral repair [35].

In this computational study, the pectopexy technique is investigated using a 3D finite element model of the female pelvic floor after hysterectomy and an implant model simulated with the mechanical mesh properties of two manufacturers. After surgery, anatomically and physiologically correct positions of the organs are obtained. Treatment outcomes, especially the vaginal-urethral axis and the organ positions are compared with the sacrocolpopexy technique [6]. The pectopexy repair using the DynaMesh®-PRP soft implant is found to stabilize the organ positions and to provide better support to the vaginal cuff after hysterectomy than the Gynemesh® and the Ultrapro® in the weaker pelvic floor with lax supporting tissues. In addition to greater bladder hypermobility below the PCL line of the Gynemesh® and the Ultrapro® as well as their critical urethral axis (Ur$\approx 34^\circ$) may lead to stress urinary incontinence using these meshes.

The models developed in this study should be employed in the future to predict potential complications such as mesh wrinkling [7], injuries, irritation or infection of adjacent organs in the pelvic and peritoneal space [36], [37]. These critical factors may lead to failures of the surgical treatment of apical prolapse and in some cases can put patients at risk for recurrence or prolapse in different compartments for which re-operation is required. Therefore, the presented computational model can be used to compare the potential success of different repair techniques and mesh implants. This may lead to a better understanding of potential postoperative complications.

Acknowledgement

The first author has been partially funded by the German Federal Ministry of Education and Research through the FHprofUnt project "BINGO", grant number 03FH073PX2. We thank Prof. M.C. Sora for the CAD model of the plastinated cross sections.

References

[1] Irvine L., Shaw R. The effects of patient obesity in gynaecological practice. *Curr Opin Obstet Gynecol*. **13**(3), 179-184, 2003.

[2] Akladios C.Y., Dautun D., Saussine C., Baldauf J.J., Mathelin C., Wattiez A. Laparoscopic sacrocolpopexy for female genital organ prolapse: establishment of a learning curve. *Eur J Obstet Gynecol Reprod Biol*. **149**(2), 218-221, 2010.

[3] Banerjee C., Noé K.G. Laparoscopic pectopexy: a new technique of prolapse surgery for obese patients. *Arch Gynecol Obstet*. **284**(3), 631-635, 2011.

[4] Noé K.G., Schiermeier S., Alkatout I., Anapolski M. Laparoscopic pectopexy: a prospective, randomized, comparative clinical trial of standard laparoscopic sacral colpocervicopexy with the new laparoscopic pectopexy–postoperative results and intermediate-term follow-up in a pilot study. *J Endourol*. **29**(2), 210-215, 2015.

[5] Cosson M., Boukerrou M., Lacaze S., Lambaudie E., Fasel J., Mesdagh H., Lobry P., Ego A. A study of pelvic ligament strength. *Eur J Obstet Gynecol Reprod Biol*. **109**(1), 80-87, 2003.

[6] Bhattarai A., Jabbari M., Anding R., Staat M. Surgical treatment of vaginal vault prolapse using different prosthetic mesh implants: a finite element analysis. *tm-Technisches Messen*. 2018. `https://doi.org/10.1515/teme-2017-0115`

[7] Bhattarai A., Staat M. Mechanics of the soft tissue reactions to different textile mesh implants. In Artmann G.M., Temiz Artmann A., Zhubanova A.A., Digel I.E. (eds). Chapter in Biological, Physical and Technical Basics of Cell Engineering. Springer, 2018. `doi: 10.1007/978-981-10-7904-7_11.`

[8] Feil P., Sora M.C. A 3d reconstruction model of the female pelvic floor by using plastinated cross sections. *Austin J Anat*. **1**(5), 4, 2014.

[9] Sora M.C., Jilavu R., Matusz P. Computer aided three-dimensional reconstruction and modeling of the pelvis, by using plastinated cross sections, as a powerful tool for morphological investigations. *Surg Radiol Anat*. **34**(8), 731-736, 2012.

[10] Bhattarai A., Frotscher R., Staat M. *Computational analysis of pelvic floor dysfunction*. In Brandão S, Da Roza T, Ramos I, Mascarenhas T (eds). Chapter in Women's Health and Biomechanics. Lecture Notes in Computational Vision and Biomechanics. Springer, Cham. **29**, 217-230, 2018. `doi:0.1007/978-3-319-71574-2_17`

[11] Rivlin R.S., Saunders D.W. Large elastic deformations of isotropic materials VII. Experiments on the deformation of rubber. *Philos Trans Royal Soc London Series A*. **243**(865), 251-288, 1951.

[12] Staat M., Trenz E., Lohmann P., Frotscher R., Klinge U., Tabaza R., Kirschner-Hermanns R. New measurements to compare soft tissue anchoring systems in pelvic floor surgery. *J Biomed Mater Res B*. **4**(100), 924–933, 2012.

[13] Rivaux G., Rubod C., Dedet B., Brieu M., Gabriel B., Cosson M. Comparative analysis of pelvic ligaments: a biomechanical study. *Int Urogynecol J*. **24**(1), 135-139, 2013.

[14] Tan T., Davis F.M., Gruber D.D., Massengill J.C., Robertson J.L., De Vita R. Histo-mechanical properties of the swine cardinal and uterosacral ligaments. *J Mech Behav Biomed Mater*. **42**, 129-137, 2015.

[15] Rubod C., Brieu M., Cosson M., Rivaux G., Clay J.C., de Landsheere L., Gabriel B. Biomechanical properties of human pelvic organs. *Urology*. **79**(4), 968.e17-968.e22, 2012.

[16] Martins P.A., Filho A.L., Fonseca A.M., Santos A., Santos L., Mascarenhas T., Jorge R.M., Ferreira A.J. Uniaxial mechanical behavior of the human female bladder. *Int Urogynecol J*. **22**(8), 991-995, 2011.

[17] Kirilova M., Stoytchev S., Pashkouleva D., Kavardzhikov V. Experimental study of the mechanical properits of human abdominal fascia. *Med Eng Phys*. **33**(1), 1-6, 2011.

[18] Bhattarai A., Staat M. Modelling of soft connective tissues to investigate female pelvic floor dysfunctions. *Comp Math Method Med*. **2018**, Article ID 9518076, 16 pages, 2018. `https://doi.org/10.1155/2018/9518076`

[19] Brandão S., Parente M., Mascarenhas T., da Silva A.R., Ramos I, Jorge R.N. Biomechanical study on the bladder neck and urethral positions: simulation of impairment of the pelvic ligaments. *J Biomech*. **48**(2), 217-223, 2015.

[20] Cobb W.S., Burns J.M., Kercher K.W., Matthews B.D., Norton H.J., Heniford B.T. Normal intraabdominal pressure in healthy adults. *J Surg Res*. **129**(2), 231-235, 2005.

[21] Petros P.E.P. The integral system. *Cent European J Urol*. **64**(3), 110-119, 2011.

[22] Olsen A.L., Smith V.J., Bergstrom J.O., Colling J.C., Clark A.L. Epidemiology of surgically managed pelvic organ prolapse and urinary incontinence. *Obstet Gynecol*. **89**(4), 501-506, 1997.

[23] Moalli P.A., Talarico L.C., Sung V.W., Klingensmith W.L., Shand S.H., Meyn L.A., Watkins S.C. Impact of menopause on collagen subtypes in the arcus tendineous fasciae pelvis. *Am J Obstet Gynecol*. **190**(3), 620-627, 2004.

[24] Gabriel B., Denschalg D., Göbel H., Fittkow C., Werner M., Gitsch G., Watermann D. Uterosacral ligament in postmenopausal women with or without pelvic organ prolapse. *Int Urogynecol J*. **16**(6), 475-479, 2005.

[25] Sederl J. Zur Operation des Prolapses der blind endigenden Scheiden. *Geburtshilfe Frauenheilkd*. **18**, 824-828, 1958.

[26] Anding R., Latz S., Müller S., Kirschner-Hermanns R. Complete extraperitoneal sacro-colpopexy with PVDF visible mesh implant. *IUGA*. 41st Annual Meeting, 2016.

[27] Beer M., Kuhn A. Surgical techniques for vault prolapse: a review of the literature. *Eur J Obstet Gynecol Reprod Biol*. **119**(2), 144-155, 2005.

[28] Demirci F., Ozdemir I., Somunkiran A., Topuz S., Iyibozkurt C., Duras Doyran G., Kemik Gul O., Gul B. Perioperative complications in abdominal sacrocolpopexy and vaginal sacrospinous ligament fixation procedures. *Int Urogynecol J Pelvic Floor Dysfunct*. **18**(3), 257-261, 2007.

[29] Silva-Filho A.L., Santos-Filho A.S., Figueiredo-Netto O., Triginelli S.A. Uncommon complications of sacrospinous fixation for treatment of vaginal vault prolapse. *Arch Gynecol Obstet*. **271**(4), 358-362, 2005.

[30] Paraiso M.F., Ballard L.A., Walters M.D., Lee J.C., Mitchinson A.R. Pelvic support defects and visceral and sexual function in women treated with sacrospinous ligament suspension and pelvic reconstruction. *Am J Obstet Gynecol*. **175**(6), 1423-1430, 1996.

[31] Flynn B.J., Webster G.D. Surgical management of the apical vaginal defect. *Curr Opin Urol*. **12**(4), 353-358, 2002.

[32] Kumar S., Malhotra N., Chumber S., Gupta P., Aruna J., Roy K.K., Sharma J.B. Control of presacral venous bleeding, using thumbtacks. *Arch Gynecol Obstet*. **276**(4), 385-386, 2007.

[33] Shiozawa T., Huebner M., Hirt B., Wallwiener D., Reisenauer C. Nerve-preserving sacrocolpopexy: anatomical study and surgical approach. *Eur J Obstet Gynecol Reprod Biol*. **152**(1), 103-107, 2010.

[34] Hefni M., El-Toukhy T., Bhaumik J., Katsimanis E. Sacrospinous cervicocolpopexy with uterine conservation for uterovaginal prolapse in elderly women: an evolving concept. *Am J Obstet Gynecol*. **188**(3), 645-650, 2003.

[35] Miklos J.R., Kohli N. Laparoscopic paravaginal repair plus burch colposuspension: review and descriptive technique. *Urology*. **56**(6 Suppl 1), 64-69, 2000.

[36] Tijdink M.M., Vierhout M.E., Heesakkers J.P., Withagen M.I.J. Surgical management of mesh-related complications after prior pelvic floor reconstructive surgery with mesh. *Int Urogynecol J*. **22**(11), 1395-1404, 2011.

[37] Bhattarai A., Frotscher R., Staat M. Biomechanical study of the female pelvic floor dysfunction using the finite element method. In Elgeti S., Simon J. (eds). Proceedings in YIC GACM III ECCOMMAS-VI GACM, 2015. URN: urn:nbn:de:hbz:82-rwth-2015-039806. `http://nbn-resolving.de/urn:nbn:de:hbz:82-rwth-2015-039806`